Journal of Experimental Botany, Vol. 75, No. 5 pp. 1601–1614, 2024
https://doi.org/10.1093/jxb/erad462 Advance Access Publication 21 November 2023

RESEARCH PAPER

Physiology, gene expression, and epiphenotype of two *Dianthus broteri* polyploid cytotypes under temperature stress

Javier López-Jurado[1,2,*], Jesús Picazo-Aragonés[1], Conchita Alonso[3], Francisco Balao[1], and Enrique Mateos-Naranjo[1]

[1] Departamento de Biología Vegetal y Ecología, Facultad de Biología, Universidad de Sevilla, Apdo. 1095, E-41080 Sevilla, Spain
[2] School of Natural Sciences, University of Tasmania, Private Bag 55, Hobart, TAS 7001, Australia
[3] Estación Biológica de Doñana, Consejo Superior de Investigaciones Científicas (CSIC), Avda. Américo Vespucio 26, E-41092 Sevilla, Spain

[*] Correspondence: javlopez@us.es

Received 29 November 2022; Editorial decision 15 November 2023; Accepted 21 November 2023

Editor: John Lunn, MPI of Molecular Plant Physiology, Germany

Abstract

Increasing evidence supports a major role for abiotic stress response in the success of plant polyploids, which usually thrive in harsh environments. However, understanding the ecophysiology of polyploids is challenging due to interactions between genome doubling and natural selection. Here, we investigated physiological responses, gene expression, and the epiphenotype of two related *Dianthus broteri* cytotypes—with different genome duplications (4× and 12×) and evolutionary trajectories—to short extreme temperature events (42/28 °C and 9/5 °C). The 12× cytotype showed higher expression of stress-responsive genes (*SWEET1*, *PP2C16*, *AI5L3*, and *ATHB7*) and enhanced gas exchange compared with 4×. Under heat stress, both ploidies had greatly impaired physiological performance and altered gene expression, with reduced cytosine methylation. However, the 12× cytotype exhibited remarkable physiological tolerance (maintaining gas exchange and water status via greater photochemical integrity and probably enhanced water storage) while down-regulating *PP2C16* expression. Conversely, 4× *D. broteri* was susceptible to thermal stress despite prioritizing water conservation, showing signs of non-stomatal photosynthetic limitations and irreversible photochemical damage. This cytotype also presented gene-specific expression patterns under heat, up-regulating *ATHB7*. These findings provide insights into divergent stress response strategies and physiological resistance resulting from polyploidy, highlighting its widespread influence on plant function.

Keywords: Cytosine methylation, gene expression, photosynthesis, polyploidy, temperature stress, water relations.

Introduction

Polyploidy [the state of organisms that have undergone whole-genome duplication (WGD)] has long been recognized as a major driver of plant evolution (Landis *et al.*, 2018; Stull *et al.*, 2021). Recent emerging evidence points out the connection between successful WGD events and periods of extinction and drastic global change (Van De Peer *et al.*, 2021). In

these scenarios, it has been widely argued that polyploids take advantage of the phenotypic novelties associated with WGD to either outcompete their diploid relatives (Rey *et al.*, 2017; Čertner *et al.*, 2019) or colonize restricted, unoccupied ecological niches (Levin and Soltis, 2018). For both possibilities, newly developed physiological traits that allow polyploids to cope with harsh environmental conditions would be essential (Maherali *et al.*, 2009; del Pozo and Ramirez-Parra, 2015). In fact, stress resistance is one of the most reported features of polyploids and certainly relies on multiple physiological characteristics. It is known that polyploidy can affect stomatal regulation (Greer *et al.*, 2017), water use and storage (Liao *et al.*, 2018), hydraulic functioning (Hao *et al.*, 2013; Losada *et al.*, 2023), or photochemical apparatus efficiency (Rakić *et al.*, 2015). Strikingly, polyploids have been repeatedly found to be not only more resistant but also more productive under optimal conditions than diploids. Larger stomata as a direct consequence of WGD frequently increase stomatal conductance and lead to higher photosynthetic rates in polyploids. Considering the growth–defence (or productivity–stress resistance) trade-off in plants (He *et al.*, 2022), the mentioned findings are counterintuitive but can be explained by the complex evolution of traits in polyploids.

After WGD, some polyploid characteristics may be further modified while others may return to a diploid-like state (Bomblies, 2020), potentially causing contrasting physiological behaviours/strategies in related polyploid cytotypes. In autopolyploids (those not involving hybridization prior to WGD), trait evolution is driven by the interaction between increased genetic diversity (via WGD and the recurrent formation of polyploid lineages; Parisod *et al.*, 2010) and epigenetic regulation (such as DNA methylation; Wang *et al.*, 2021), and are ultimately enhanced by local adaptation processes (Maherali *et al.*, 2009; Domínguez-Delgado *et al.*, 2021). Although gene expression is thought to increase linearly in autopolyploids at the cell level (transcripts per cell; Stupar *et al.*, 2007), individual gene dosage responses normally decrease this number (Doyle and Coate, 2020). In addition, the aforementioned factors—especially epigenetic regulation—are known to modify transcription, and evidence of both minor gene expression changes and large differences between diploids and autopolyploids have been reported (Spoelhof *et al.*, 2017). These transcriptome alterations are proposed to be associated with the differential expression of homoeologues under contrasting environmental conditions (Madlung and Wendel, 2013), which often acts through molecular mechanisms (e.g. transposable elements; Baduel *et al.*, 2019). However, changes in gene expression and regulatory networks are largely unexplored in relation to additive genome duplications such as those found in large polyploid complexes with high-order ploidy levels.

Among the environmental factors shaping polyploid evolution, temperature is probably the most influential one by affecting fundamental processes such as the formation of unreduced gametes (Ramsey and Schemske, 1998), the superiority of polyploids for niche colonization (Moura *et al.*, 2021), and their global biogeography (Rice *et al.*, 2019). Thus, comparing the response of related polyploid plants to extreme temperatures is crucial for two reasons: (i) to shed light on the functional drivers of the evolutionary adaptations that allowed those lineages to establish and thrive; and (ii) to predict their future performance under global change scenarios. This second point becomes especially relevant in regions such as the Mediterranean, where unprecedented extreme temperature events have been documented over recent years (both cold and heat waves; Scaife and Knight, 2008; García-Herrera *et al.*, 2010; Sánchez-Benítez *et al.*, 2018) and are predicted to occur earlier as well as to be more frequent and intense throughout the 21st century (Giorgi and Lionello, 2008; Grassi *et al.*, 2013; Lau and Nath, 2014), especially in the Iberian Peninsula (Fonseca *et al.*, 2016; Abaurrea *et al.*, 2018).

Endemic to this area, the autopolyploid *Dianthus broteri* complex (*Caryophyllaceae*) is an excellent system to investigate the modification of physiological tolerances to temperature with WGD and subsequent evolutionary changes. It comprises four different cytotypes, namely 2×, 4×, 6×, and 12×, with non-overlapping geographic distributions in Spain and Portugal (Balao *et al.*, 2009). The two higher ploidies of this endemic perennial herb (6× and 12×) inhabit divergent and narrow environmental niches, whereas the lower cytotypes (2× and 4×) occur in broader areas with overall more benign conditions (López-Jurado *et al.*, 2019a). Tetraploids and dodecaploids in particular appear in the most distant niches regarding their environments and show alternative niche evolution patterns (expansion and contraction, respectively). The 4× cytotype showed the highest niche breadth, occupying three disjunct distribution areas (Supplementary Fig. S1) and encompassing many different bioclimatic and edaphic conditions. By contrast, *Dianthus inoxianus* (the 12× cytotype) has a single and small distribution range in SW Spain (Supplementary Fig. S1), characterized by an extreme Mediterranean climate with hot summers and severe as well as prolonged drought events (Balao *et al.*, 2009; López-Jurado *et al.*, 2019a). Moreover, these opposed distribution patterns are ultimately explained by their different evolutionary histories: the tetraploids originated from two separate polyploidization events and the dodecaploids from only one, and have independently evolved regarding the other cytotypes (Balao *et al.*, 2010).

In addition to their divergent origins and ecological niches, *D. broteri* cytotypes also present variation in multiple morphological (Balao *et al.*, 2011) and functional traits (López-Jurado *et al.*, 2022) as well as in the percentage of genome-wide cytosine methylation that characterizes their epiphenotype (Alonso *et al.*, 2016a). Such multidimensional variance on the (epi)phenotype may explain previous results on shifts in stress physiology among cytotypes. We have described immediate and posterior effects of WGD on gas exchange and chlorophyll fluorescence by comparing diploids, natural and synthetic tetraploids (Domínguez-Delgado *et al.*, 2021), as well as marked

divergent photochemical responses under severe heat in the 6× and 12× cytotypes (López-Jurado *et al.*, 2020). Regarding the highest order ploidy, previous studies indicate a distinct leaf economics spectrum (López-Jurado *et al.*, 2022) and a high tolerance and recovery capacity to water shortage (López-Jurado *et al.*, 2016) as well as to stresses associated with transplant shock (López-Jurado *et al.*, 2019b).

Considering this background, our aim was to shed light on the potential of polyploidy to promote different plant tolerance strategies to cope with temperature stress, particularly in the 12× cytotype with a very narrow distribution range. Here, we pursued this goal by unravelling the physiological responses and their underlying gene expression and epigenetic shifts of two *D. broteri* polyploid cytotypes to short heat and cold treatments. To our knowledge, only a few studies have investigated the impact of these extreme events on plant ecophysiology (e.g. Duarte *et al.*, 2015a, b; Pérez-Romero *et al.*, 2019), but none of them has compared their effects between polyploid relatives, which will help to explain possible consequences of WGD beyond duplication from a diploid to a tetraploid genome. Based on previous information, we hypothesize that the 12× cytotype has developed specific physiological responses to heat stress (enabled by WGD and natural selection in harsh environments) that allow it to better resist the imposed acute climate events compared with its 4× counterpart, that has the widest distribution within this complex.

Materials and methods

Plant material and experimental set-up

Tetraploid (4×) and dodecaploid (12×) *Dianthus broteri* cuttings and/or seeds were collected from three natural populations of each ploidy level (Supplementary Fig. S1). After seedling emergence and rooting of cuttings, *D. broteri* plants were sown in 2.5 litre pots containing organic commercial substrate (Gramoflor GmbH und Co. KG) and perlite mixture (3:1), and placed inside a glasshouse (University of Seville) until the beginning of the experiment. Controlled conditions were air temperature of 21–25 °C, relative humidity of 40–60%, and maximum photosynthetic photon flux density (PPFD) incident on leaves of 1200 µmol m^{-2} s^{-1}.

In February 2018, mature and well-irrigated plants of similar size were acclimated to control temperature (20/18 °C) in controlled-environment chambers (Aralab/Fitoclima 18.000EH, Lisbon, Portugal) for 1 week. Then, they were randomly divided into three blocks of 10 individuals per ploidy level corresponding to three different temperature treatments (day/night): cold (9/5 °C), control (20/18 °C), and heat (42/28 °C). Cold and heat treatments were selected based on short extreme temperature events recorded in recent years along the southern Iberian Peninsula, where natural populations of both *D. broteri* cytotypes occur (López-Jurado *et al.*, 2019a). The climate chambers were programmed with an alternating diurnal regime of 16/8 h day/night rhythm, 50 ± 5% relative humidity, and a maximum PPFD of 300 µmol photon m^{-2} s^{-1}. Furthermore, the soil water content was maintained at field capacity during the experiment.

Plants were exposed for 48 h to each temperature regime. Measurements of leaf water status, gas exchange, chlorophyll fluorescence, and concentration of photosynthetic pigments were taken immediately after that to assess plant responses to stress. Estimates of long-term fitness consequences of the treatments were not feasible because plants did not reach the reproductive stage until ~1 year of growth, and it was not possible to keep them that long under homogeneous controlled conditions.

Leaf water status

Leaf water potential, Ψ_w, osmotic potential, Ψ_o, and relative water content, RWC, were measured at midday on random fully developed leaves of both cytotypes subjected to each specific temperature range treatment (n=5). Ψ_w is the simplest and most widely employed indicator of leaf hydration and overall water status. Ψ_o is a component of the latter used to check for osmotic adjustment in plants (Ψ_o drops under stress in response to dehydration), a process caused by the accumulation of osmoprotectants in cells in order to avoid irreversible turgor loss. RWC was included as an integrated metric of water pools in plant tissues (accounting for water supply and retention but also water demand; Martinez-Vilalta *et al.*, 2019).

Ψ_w was measured using a pressure chamber (Model 1515 D; Pressure Chamber Instruments, PMS), while Ψ_o was determined by freezing small segments of leaf tissue in liquid nitrogen, letting them thaw, and centrifuging (12 000 *g*, 10 min) at 4 °C in 2 ml tubes. To separate a minimum of 10 µl of leaf sap, we inserted the top of the filter tips into these tubes (Pérez-Romero *et al.*, 2020). Ψ_o was measured in the extracted sap using the psychrometric technique with a vapour pressure osmometer (5600 Vapro, Wescor, Logan, UT, USA). Finally, the RWC was calculated as follows:

$$\mathrm{RWC}\,(\%) = [(\mathrm{FW} - \mathrm{DW}) / (\mathrm{TW} - \mathrm{DW})] \times 100$$

where FW was the leaf fresh weight, DW was the leaf dry weight after drying at 60 °C until constant weight was reached, and TW was the leaf saturated weight after 24 h rehydration in distilled water at 4 °C in darkness to minimize respiration losses.

Leaf gas exchange

Instantaneous gas exchange measurements were taken in fully developed and randomly selected leaves from each experimental combination of temperature range and ploidy level (n=10), using an infrared gas analyser in an open system (LI-6400XT, Li-Cor Inc., Lincoln, NE, USA) equipped with a light leaf chamber (Li-6400-02B, Li-Cor Inc.). Net photosynthetic rate (A_N), stomatal conductance (g_s), intercellular CO_2 concentration (C_i), and intrinsic water use efficiency ($_i$WUE) were recorded under the following leaf chamber settings: PPFD of 1500, 1000, and 300 µmol m^{-2} s^{-1} (with 15% blue light to maximize stomatal aperture), air relative humidity of 50 ± 2%, CO_2 concentration surrounding the leaf (C_a) of 400 µmol CO_2 mol^{-1}, and temperature of 9, 20, and 42 °C for plants grown in low, medium, and high temperature ranges, respectively. Vapour pressure deficit (VPD) inside the leaf chamber varied with the different temperature regimes (cold, 0.9 ± 0.1 kPa; control, 1.7 ± 0.2 kPa; heat, 5.7 ± 0.6 kPa). For all measurements, the leaf area enclosed in the chamber was determined by scanning to obtain images, which were used for leaf area evaluation and gas exchange measurement recalculation.

Chlorophyll fluorescence

Light- and dark-adapted chlorophyll fluorescence parameters were quantified in leaves of each temperature range treatment and ploidy level combination (n=10) at dawn (stable, 50 µmol m^{-2} s^{-1} ambient light) and at midday (1400 µmol m^{-2} s^{-1}). The saturation pulse method, as described in Schreiber *et al.* (1986), was followed using a portable modulated fluorimeter (FMS-2, Hansatech Instruments Ltd, UK). In short, leaves were dark or light adapted for 30 min and then saturated by applying an actinic light pulse of 10 000 µmol m^{-2} s^{-1} for 0.8 s. The obtained fluorescence

parameters were employed to calculate the maximum quantum efficiency of PSII photochemistry (F_v/F_m), quantum efficiency of PSII (Φ_{PSII}; Genty *et al.*, 1989), and non-photochemical quenching (NPQ). F_v/F_m reflects the efficiency of PSII if all reaction centres were open and can be used as an index of temperature-induced injury in leaves; Φ_{PSII} indicates the proportion of absorbed energy that is used for photochemical processes; and NPQ measures thermal dissipation of excess light energy as a photoprotective mechanism. Additionally, chronic (PI_{chr}) as well as dynamic (PI_{dyn}) photoinhibition were calculated with the values obtained at dawn and midday in accordance with Werner *et al.* (2002), as:

$$PI_{chr} = \frac{(F_v/F_m)_{max} - (F_v/F_m)_d}{(F_v/F_m)_{max}} \times 100$$

$$PI_{dyn} = \frac{(F_v/F_m)_d - (F_v/F_m)_{mid}}{(F_v/F_m)_{max}} \times 100$$

where $(F_v/F_m)_d$ and $(F_v/F_m)_{mid}$ are the dawn and midday F_v/F_m values, respectively. $(F_v/F_m)_{max}$ is the maximum F_v/F_m value, which was calculated as the average of dawn measurements of the control treatment.

Leaf photosynthetic pigment concentrations

Leaf samples were randomly collected (n=5, for each temperature range treatment and ploidy level combination), flash-frozen in liquid N_2, and freeze-dried for 48 h in darkness to prevent photodegradation processes for photosynthetic pigment concentration analysis (Duarte *et al.*, 2015a). Leaves were then ground in pure acetone and pigments were extracted at –20 °C for 24 h in the dark. These samples were centrifuged (2000 *g*, 15 min) at 4 °C and the resulting supernatant scanned in a dual beam spectrophotometer (DU-8800DS, Shanghai Drawell Scientific Instrument Co., Ltd, China) from 350 nm to 750 nm in 1 nm steps. The consequent absorbance spectrum was used for pigment quantification by introducing it in a Gauss-Peak Spectra (GPS) fitting library, using SigmaPlot Software (Küpper *et al.*, 2007). The de-epoxidation state index (DES) was calculated as:

$$DES = ([Violaxanthin] + [Anteroxanthin]) / ([Violaxanthin] + [Anteroxanthin] + [Zeaxanthin])$$

Expression of stress-responsive genes and global cytosine methylation

Gene expression analysis was conducted on *D. broteri* using quantitative real-time PCRs (RT-qPCRs). We tested eight genes (*AI5L3*, *ATHB7*, *PP2C16*, *SWEET1*, *MYB39*, *SEP2*, *TIL*, and *PTR33*) that were differentially expressed in response to thermal stress in the related species *Dianthus spiculifolius* (Zhou *et al.*, 2017; Supplementary Table S1). RNA was extracted from leaves and isolated using the Direct-zol RNA Miniprep commercial kit (Zymo Research, Irvine, CA, USA), then reverse transcribed into cDNA (three technical replicates per sample) using the iScript cDNA synthesis kit (Bio-Rad, Hercules, CA, USA). All qPCRs were carried out using a LightCycler® 480 Instrument II (Roche Molecular System, Germany) as described in Kolouškova *et al.* (2017): denaturation step at 95 °C for 5 min, followed by 55 amplification and quantification cycles at 95 °C for 10 s, 60 °C for 10 s, and 72 °C for 15 s. The efficiency of each primer was calculated by performing a qPCR analysis of a cDNA sample diluted through a series of 1:2 covering seven dilution points with a starting cDNA amount of 50 ng.

For genes that showed enough efficiency (>85%) for qPCR differential expression analysis, differences in efficiency between ploidy levels were analysed following an analysis of covariance (ANCOVA) approach. We compared the slopes (which were used to calculate efficiency) between cytotypes, representing the variation of the crossing point (Cp) at different concentrations of cDNA on a logarithmic scale. The resulting *P*-values were corrected for false discovery rate (FDR). Additionally, the *TIF5A* gene (Yu *et al.*, 2021) was used as reference for normalization in both cytotypes since it shows stable expression among ploidy levels in *D. broteri* (Rodríguez-Parra *et al.*, 2022). After successfully passed the efficiency test, three biological replicates per sample were analysed for each studied gene and treatment in both cytotypes (4× and 12×).

Furthermore, the genome-wide percentage cytosine methylation was estimated by HPLC (Alonso *et al.*, 2016b) for the two cytotypes at 20/18 °C and 42/28 °C (n=8 for each temperature range treatment and ploidy level combination). Only the heat treatment was included as the extreme temperature range because it showed the overall greatest differences between cytotypes for most variables. Total genomic DNA from leaves of control and high temperature treatments was extracted using a Qiagen DNeasy Plant Mini Kit, and subsequently digested with DNA Degradase Plus™ (Zymo Research, Irvine, CA, USA). Two independent replicates of digested DNA per sample were processed to estimate global cytosine methylation. DNA cytosine methylation was determined for each sample by reversed phase HPLC with spectrofluorimetric detection. The percentage of total cytosine methylation in each replicated sample was estimated at 100 × 5mdC/(5mdC+dC), where 5mdC and dC are the integrated areas under the peaks for 5-methyl-2'-deoxycytidine and 2'-deoxycytidine, respectively.

Statistical analyses

All statistical analyses were performed in R software v.4.0.3 (R Core Team, 2020). Generalized linear models (GLMs; two-way ANOVAs) were used to analyse the interactive effects of temperature range and ploidy level (as fixed categorical factors) on the different parameters (as response variables) evaluated for *D. broteri*. Tukey's post-hoc HSD tests (α=0.05) were used to detect pairwise differences between groups (i) whenever the interaction ploidy×temperature had a significant effect, or (ii) in cases where temperature was significant but the interaction was not. The Shapiro–Wilk test was used to check the normality of model residuals for each variable, and no departure was observed for the reported models.

The gene expression data obtained from the RT-qPCR experiment were analysed using the MCMC.qpcr R package v.1.2.4. (Matz, 2020). This package implements a Poisson-lognormal generalized mixed model using Markov chain Monte Carlo (MCMC; Matz *et al.*, 2013). Expression changes for the four genes were estimated from the joint posterior distribution of parameters. Ploidy level and temperature treatments were used as fixed factors, while *TIF5A* (Yu *et al.*, 2021; Rodríguez-Parra *et al.*, 2022) was used as a reference gene for soft normalization of gene expression prior to the model function to account for variations in cDNA, allowing up to 1.2-fold changes. Furthermore, the variation in global cytosine methylation was analysed using linear mixed models (LMMs) in the lme4 R package v.1.1.27.1 (Bates *et al.*, 2015), employing the individual as random factor and ploidy and temperature as fixed factors. Individual was entered as a random effect to account for non-independence of the replicated analyses. The consistency of the replicated analyses (i.e. the intraclass correlation coefficient) was 0.801.

Results

Leaf water status

There was a significant interaction between temperature treatment and ploidy level for the RWC of *D. broteri* at the end

of the experiment (GLM: temperature×ploidy, $F_{2,22}$=4.83, P<0.05; Fig. 1A). Therefore, RWC values tended to decrease in plants exposed to 42/28 °C for both cytotypes, but this reduction was only significant for tetraploid individuals (from 80.61 ± 5.80% under control conditions to 52.90 ± 5.24% under heat treatment). In addition, Ψ_w decreased with heat and cold shocks independently of the ploidy level, exhibiting values around −1.0 MPa (GLM: temperature, $F_{2,17}$=35.38, P<0.001; Fig. 1B). A similar trend was recorded for Ψ_o, but only heat significantly affected Ψ_o values compared with those of the control treatment (GLM: temperature, $F_{2,22}$=20.07, P<0.001; Fig. 1C).

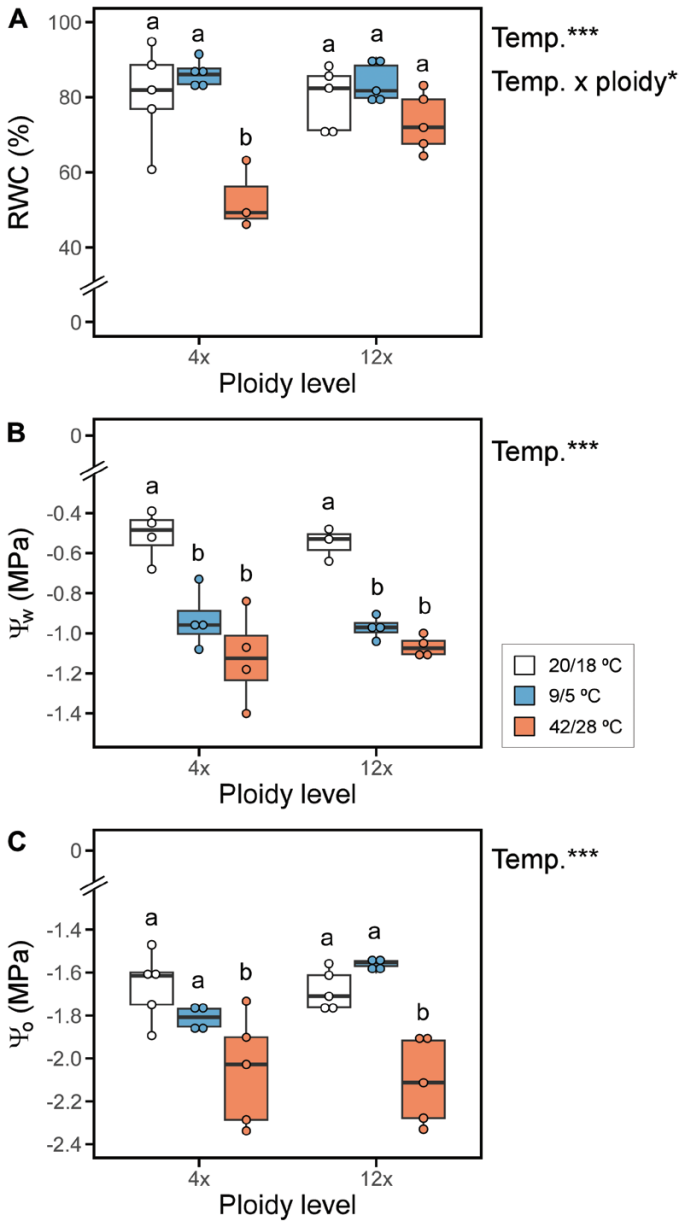

Fig. 1. Relative water content, RWC (A), leaf water potential, Ψ_w (B), and osmotic potential, Ψ_o (C), in 4× and 12× *Dianthus broteri* after exposure to three different temperature range treatments (9/5, 20/18, and 42/28 °C) for 48 h. Both raw data points and box plots are displayed. In the latter, horizontal lines depict the median, and boxes and whiskers represent the interquartile range and the non-outlier ranges, respectively (n=5). Different letters indicate means that are significantly different from each other (GLM: P<0.05, Tukey's HSD test: α=0.05). Asterisks next to factors indicate their level of significance in the model (*P<0.05, **P<0.01, ***P<0.001).

Leaf gas exchange

Both the temperature treatment and ploidy level affected gas exchange in *D. broteri*, especially at high PPFD (i.e. 1500 µmol photon m^{-2} s^{-1}; Fig. 2). Compared with plants in the control temperature regime (20/18 °C), A_N tended to decrease in plants subjected to both extreme temperatures. This effect was especially marked under the heat treatment and particularly for the 4× cytotype, which showed negative A_N values (GLM: temperature, P<0.001; ploidy, P<0.05; Fig. 2A; Supplementary Fig. S2A, B) regardless of the PPFD used (i.e. 1500, 1000, or 300 µmol m^{-2} s^{-1}). Similarly, g_s of tetraploid plants was negatively affected by heat (GLM: temperature, P<0.05). However, this extreme temperature range had no effect on g_s of their dodecaploid counterparts, which did not drop below the 50 mmol H_2O m^{-2} s^{-1} threshold (Fig. 2B). Temperature also severely affected C_i of *D. broteri* individuals (GLM: temperature, P<0.001). Oppositely to A_N and g_s, C_i was overall higher in plants exposed to both extreme temperature ranges, with this effect again being more marked in 4× individuals under 42/28 °C, which showed the highest C_i values at the three different PPFDs (~400 µmol CO_2 mol^{-1}; Fig. 2C; Supplementary Fig. S2E, F). Finally, $_i$WUE was only significantly affected by temperature (GLM: temperature, P<0.001), under both cold and heat treatments. Again, the reduction was more pronounced at 42/28 °C, given that no differences were detected between control and cold temperature regimes for the 12× cytotype at high PPFD (Fig. 2D). It is noteworthy that $_i$WUE was not detected in tetraploid plants subjected to the heat treatment due to the negative A_N values recorded under this condition, as we stated earlier (Fig. 2D).

Chlorophyll fluorescence

Dianthus broteri cytotypes exhibited significantly different values of chlorophyll fluorescence parameters, which were also affected by cold and heat treatments (Fig. 3). F_v/F_m showed higher average values in the 12× cytotype compared with the 4× (GLM: ploidy, $F_{1,51}$=5.25, P<0.05) regardless of temperature, but especially under heat and cold (Fig. 3A). Nevertheless, both cytotypes experienced a decrease in F_v/F_m after exposure to the two extreme temperature ranges (GLM: temperature, $F_{2,51}$=31.56, P<0.001; Fig. 3A). In a similar fashion, Φ_{PSII} was higher in 12× *D. broteri* (GLM: ploidy, $F_{1,46}$=20.02, P<0.001; Fig. 3B) and also decreased with both extreme temperature ranges (GLM: temperature, $F_{2,46}$=108.31, P<0.001), but heat especially impaired Φ_{PSII} in 4× *D. broteri*

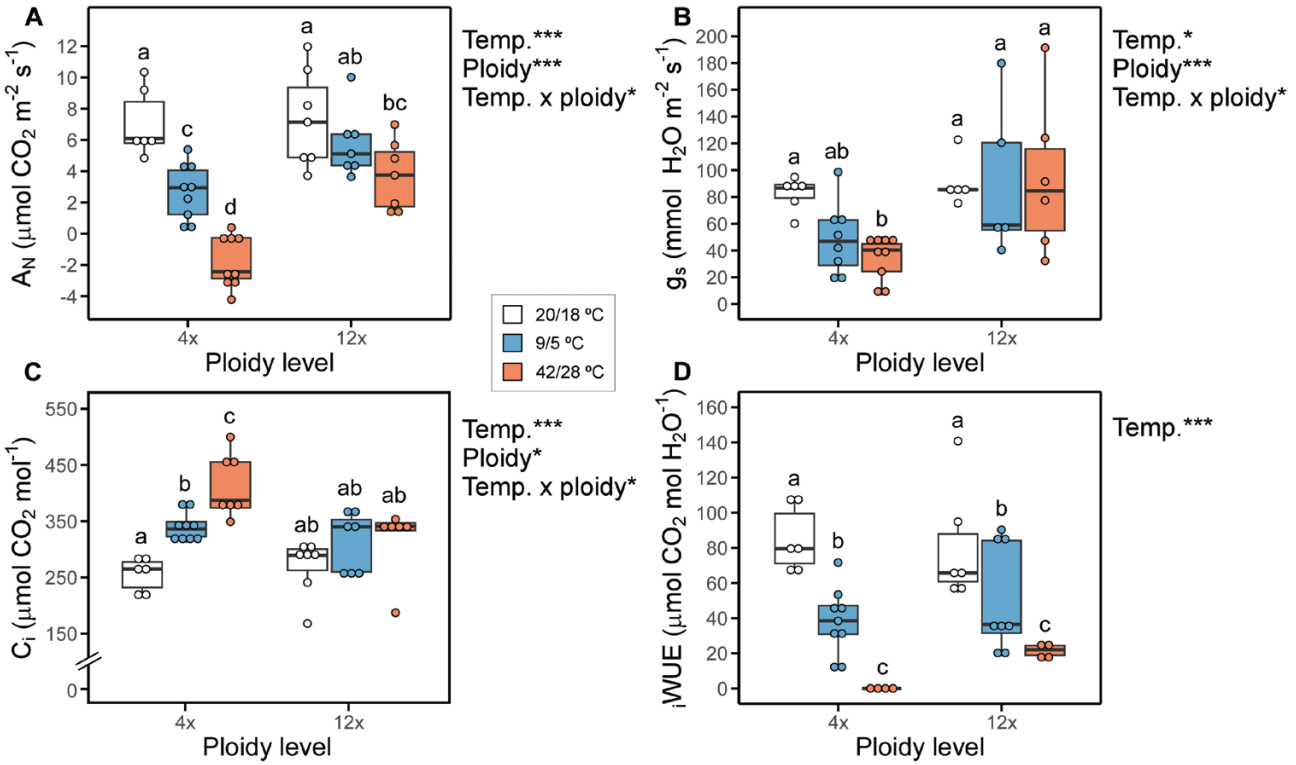

Fig. 2. Net photosynthetic rate, A_N (A), stomatal conductance, g_s (B), intercellular CO_2 concentration, C_i (C), and intrinsic water use efficiency, ¡WUE (D), in 4× and 12× *Dianthus broteri* after exposure to three different temperature range treatments (9/5, 20/18, and 42/28 °C) for 48 h. Parameters were recorded at a PPFD of 1500 µmol m^{-2} s^{-1}. Both raw data points and box plots are displayed. In the latter, horizontal lines depict the median, and boxes and whiskers represent the interquartile range and the non-outlier ranges, respectively (n=10). Different letters indicate means that are significantly different from each other (GLM: P<0.05, Tukey's HSD test: α=0.05). Asterisks next to factors indicate their level of significance in the model (*P<0.05, **P<0.01, ***P<0.001).

(GLM: temperature×ploidy, $F_{2,46}$=9.79, P<0.001; Fig. 3B). Oppositely to F_v/F_m and Φ_{PSII}, NPQ was higher in tetraploids than in dodecaploids overall (GLM: ploidy, $F_{1,36}$=10.02, P<0.01; Fig. 3C). Although both cytotypes showed increased NPQ under the temperature extremes (GLM: temperature, $F_{2,36}$=19.61, P<0.001), the average rise compared with the control treatment was also higher for tetraploids (416.39% increase versus 259.64% for dodecaploids). Comparing the impact of heat and cold shocks, NPQ was more greatly enhanced by the former in both ploidies. This was especially evident for 12× *D. broteri* given that the cold temperature treatment did not even alter its control values significantly (GLM: temperature×ploidy, $F_{2,36}$=2.59, P<0.1; Fig. 3C).

Compared with the control temperature range, the percentage of total photoinhibition increased with heat and cold treatments in both tetraploid and dodecaploid *D. broteri* plants (Fig. 3D). Overall, the 4× cytotype was more photoinhibited after exposure to both temperature extremes than the 12× cytotype. Chronic photoinhibition was higher in tetraploids, whereas dynamic photoinhibition barely varied between ploidies (Fig. 3D). Notably, the rise of chronic photoinhibition was more pronounced under heat (average 13.24% increment at 42/28 °C versus 3.74% increment at 9/5 °C), but the opposite trend was found for dynamic photoinhibition (average 5.40% increment at 42/28 °C versus 21.50% increment at 9/5 °C).

Leaf photosynthetic pigment concentrations

Photosynthetic pigment contents in *D. broteri* leaves were overall highly variable in both cytotypes, and temperature had a weaker influence on them than on the previously described parameters. A significant effect of ploidy was found for the total content of chlorophylls (Chl *a*+*b*) and for Chl *b*, with the 12× cytotype being the one showing more elevated concentrations over all temperatures (Chl *a*+*b*, GLM: ploidy, $F_{1,44}$=3.32, P<0.1; Chl *b*, GLM: ploidy, $F_{1,44}$=4.60, P<0.05; Table 1). Similarly, 12× *D. broteri* exhibited higher neoxanthin and zeaxanthin concentrations compared with the 4× cytotype (GLM: ploidy, P<0.001; Table 1). Also regarding xanthophylls, dodecaploids were able to maintain violaxanthin stable at the three temperature ranges, while average values decreased under temperature extremes for tetraploids (GLM: temperature×ploidy, $F_{2,43}$=2.97, P<0.1; Table 1).

Finally, the pigment DES index was higher for the 4× cytotype compared with its 12× counterpart (GLM: ploidy, $F_{1,44}$=13.51, P<0.001; Table 1).

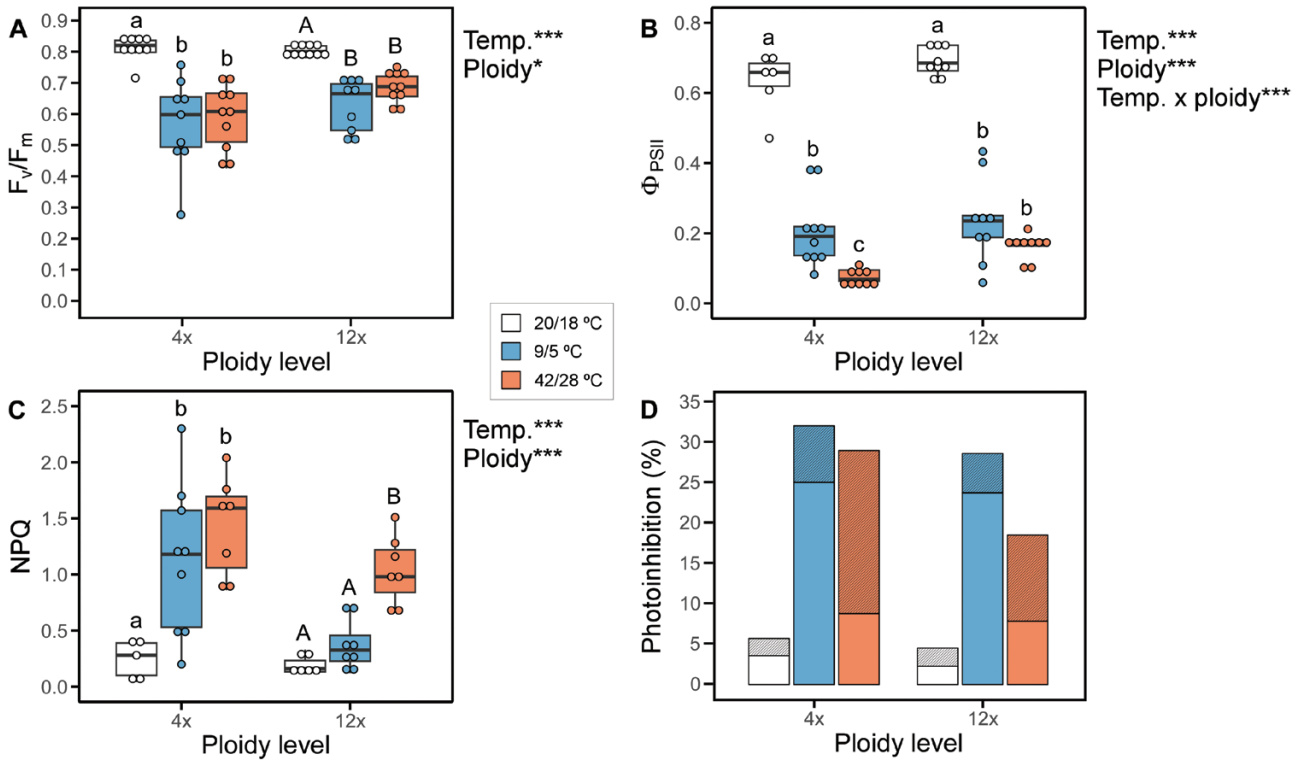

Fig. 3. Maximum quantum efficiency of PSII photochemistry, F_v/F_m (A), quantum efficiency of PSII, Φ_{PSII} (B), non-photochemical quenching, NPQ (C), and total photoinhibition percentage (D), in 4× and 12× *Dianthus broteri* after exposure to three different temperature range treatments (9/5, 20/18, and 42/28 °C) for 48 h. Both raw data points and box plots are displayed. In the latter, horizontal lines depict the median, and boxes and whiskers represent the interquartile range and the non-outlier ranges, respectively (n=10). Different letters indicate means that are significantly different from each other (GLM: P<0.05, Tukey's HSD test: α=0.05). In cases where there are significant individual effects of temperature and ploidy but not of their interaction temperature×ploidy, a different set of letters (upper and lower case) is displayed for each cytotype. Asterisks next to factors indicate their level of significance in the model (*P<0.05, **P<0.01, ***P<0.001). Dynamic and chronic photoinhibition are shown with plain and striped bars, respectively.

Expression of stress-related genes and epigenomic changes

Moderate levels of qPCR cross-amplification were observed in *D. broteri* for the eight stress-related genes obtained from *D. spiculifolius* (Supplementary Table S1). Only four genes (*AI5L3*, *ATHB7*, *PP2C16*, and *SWEET*) had sufficient efficiency in both cytotypes (4× and 12×). All four genes demonstrated comparable efficiencies between ploidy levels (P<0.05; Supplementary Table S1). Inter-cytotype differences in relative expression were detected for the four selected genes involved in abiotic stress response (ploidy, P_{MCMC}<0.05). The 12× cytotype always showed a higher average transcript abundance compared with the 4× (Fig. 4). In terms of temperature effect, the 9/5 °C range did not change the expression of any gene compared with control values. In turn, the direction of the changes in gene expression under 42/28 °C was gene specific. In *SWEET1*, the high temperature treatment decreased expression levels in both cytotypes (temperature, P_{MCMC}<0.001), while the transcripts of *PP2C16* only decreased for the 12× cytotype (temperature×ploidy, P_{MCMC}<0.05; Fig. 4A, B). In contrast, the expression of *ATHB7* increased in 4× plants exposed to heat (temperature×ploidy, P_{MCMC}<0.01; Fig. 4D). Finally, the expression of *AI5L3* did not change with temperature treatments (Fig. 4C).

Moreover, global cytosine methylation in *D. broteri* leaves ranged between 23.75% and 38.42% (average 29.62 ± 0.41%) and did not vary between the two cytotypes (LMM: ploidy, $F_{1,16}$=0.12, P=0.73). The heat treatment significantly decreased the percentage of cytosine methylation to 2% (LMM: temperature, $F_{1,16}$=19.22, P<0.001; Fig. 5), and that effect was similar for the two cytotypes (temperature×ploidy, $F_{1,16}$=0.06, P=0.80).

Discussion

In this study, as expected, physiological performance was generally impaired for both *D. broteri* cytotypes immediately after exposure to short extreme low and high temperatures events, the latter affecting more traits and usually having stronger short-term effects. Interestingly, the extent of this impact differed between 4× and 12× *D. broteri*, with the latter exhibiting greater early tolerance through a suite of coordinated physiological traits.

Table 1. Leaf photosynthetic pigment concentrations (μg g^{-1}) and de-epoxidation state (DES) in 4× and 12× *Dianthus broteri* after exposure to three different temperature range treatments (9/5, 20/18, and 42/28 °C) for 48 h.

Temperature (°C)	Ploidy	Chl *a*	Chl *b*	Total Chls	N	V	Z	DES
9/5	4×	511 ± 62	260 ± 23	771 ± 83	24.8 ± 3.9 a	20.7 ± 1.7 a	29.3 ± 3.2 a	0.48 ± 0.04
	12×	662 ± 93	285 ± 30	948 ± 121	44.8 ± 4.8 A	22.8 ± 3.9 ab	79.5 ± 25.6 b	0.29 ± 0.05
20/18	4×	728 ± 115	292 ± 48	1020 ± 161	34.8 ± 10.1 a	37.9 ± 9.6 b	40.6 ± 4.7 ab	0.46 ± 0.06
	12×	639 ± 162	315 ± 41	954 ± 197	67.5 ± 8.3B	18.3 ± 8.1 a	37.0 ± 5.1 ab	0.24 ± 0.10
42/28	4×	497 ± 55	227 ± 23	723 ± 75	32.7 ± 5.9 a	22.1 ± 3.2 a	34.3 ± 4.8 a	0.45 ± 0.05
	12×	662 ± 56	321 ± 28	982 ± 79	55.5 ± 8.8 AB	23.9 ± 3.8 ab	53.6 ± 10.0 ab	0.36 ± 0.04
Significant effects			Ploidy*	Ploidy•	Ploidy***	Temp. × ploidy•	Ploidy*	Ploidy***
					Temperature•		Temp. × ploidy•	

N, neoxanthin; V, violaxanthin; Z for zeaxanthin.
Values represent the mean ±SE error, *n*=5. Different letters indicate means that are significantly different from each other (GLM: $P<0.1$, Tukey's HSD test: α=0.1). In cases where there are significant individual effects of temperature and ploidy but not of their interaction temperature×ploidy, a different set of letters (upper and lower case) is displayed for each cytotype. Symbols next to factors indicate their level of significance in the model (•$P<0.1$, *$P<0.05$, **$P<0.01$, ***$P<0.001$).

Water relations and photosynthetic performance

Despite appropriate watering of plants during the experiment, extreme temperatures are known to cause desiccation symptoms in plant function (Pintó-Marijuan and Munné-Bosch, 2013) and then lower leaf water potential (Ψ_w) to maintain water supply, which was experienced by both cytotypes under heat and cold (Fig. 1). Such conditions also encourage water retention, which was promoted by the drop in osmotic potential (Ψ_o; i.e. osmotic adjustment) for plants exposed to the heat treatment, so this temperature extreme impacted plant water relations more severely in *D. broteri*. Although the trends detected in Ψ_w and Ψ_o were similar for both cytotypes under temperature stress, overall water status differed. Dodecaploid *D. broteri* was able to maintain control values of RWC at high temperatures, which would rely on a higher hydraulic capacitance, allowing the plant to buffer water potential fluctuations. This finding has been previously described in tetraploid apple trees compared with diploid cultivars (De Baerdemaeker *et al.*, 2018) and could be explained by a greater ability of polyploids to store water in a tissue (leaves in this case), an ultimate consequence of WGD-driven increased cell size and lowered cell surface area:volume ratio (Pacey *et al.*, 2022).

Furthermore, 12× *D. broteri* was able to maintain stomatal opening and keep positive assimilation rates under temperature extremes (Fig. 2). Contrary to empirical evidence suggesting that stomatal conductance (g_s) declines in response to high VPD (temperature-driven in this experiment; Grossiord *et al.*, 2020), this ploidy showed a remarkably tolerant behaviour under these conditions by means of unaltered leaf water balance. This matches the resource-acquisitive functional strategy described for this cytotype (López-Jurado *et al.*, 2022), which would benefit from the use of stored water to not decrease photosynthesis if stress-induced damage is reversible (similarly to results reported by Li *et al.* (1996). Moreover, keeping stomata open when experiencing thermal stress, especially heat, could reduce physiological damage due to the evaporative cooling of leaves (Schymanski *et al.*, 2013), at least when water is available. In contrast, tetraploids prioritized stomatal closure to prevent water loss in response to thermal stress. Smaller, more densely packed stomata in 4× (Balao *et al.*, 2011) would enable this behaviour by permitting their faster adjustment to the changing environment (Lawson and Vialet-Chabrand, 2019). Nevertheless, our results do not support that decreased g_s was causing reduced assimilation rates (A_N) in 4× *D. broteri*, since CO_2 was highly concentrated in the intercellular space (C_i) after heat and cold treatments. Therefore, other limitations to photosynthesis would be acting in 4× plants, namely mesophyll or biochemical. Higher mesophyll resistance in tetraploids would cause a drawdown of CO_2 from the intercellular space to the chloroplast stroma and hence explain the decline in A_N (Mizokami *et al.*, 2019). Alternatively, thermal stress may cause Rubisco deactivation and affect other enzymes related to carbon assimilation, leading to impaired carboxylation capacity (Hendrickson *et al.*, 2004; Sage *et al.*, 2008; Scafaro *et al.*, 2016). Although our experimental design does not allow us to ascertain which possibility has a larger impact, the higher degree of photoinhibition and loss of PSII efficiency in tetraploids (see below) suggest significant damage to their photosynthetic system.

Integrity of the photosynthetic system and photochemical adaptations

High integrity of the photosynthetic machinery under drought was demonstrated in a previous study for 12× *D. broteri* (López-Jurado *et al.*, 2016). Here, greater photochemical integrity compared with 4× *D. broteri* was confirmed in response to thermal stress (Fig. 3). Although photosynthetic performance was compromised for both cytotypes, particularly after the heat shock, higher photochemical efficiency (F_v/F_m and Φ_{PSII}) and less photoinhibition explain the slightly lower drop in A_N for dodecaploids. In line with that, the 12× cytotype also presented greater concentrations of total chlorophylls (Table 1), which

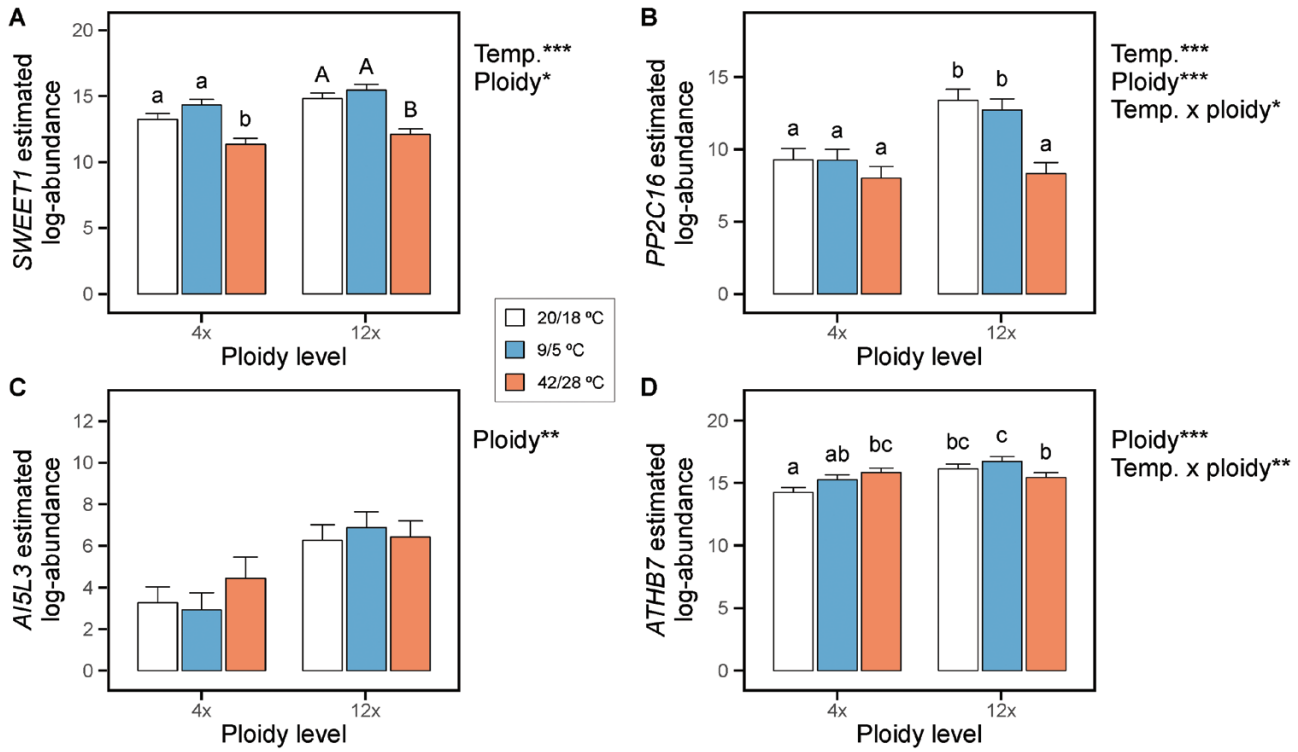

Fig. 4. Transcript abundance of stress-responsive genes *SWEET1* (A), *PP2C16* (B), *AI5L3* (C), and *ATHB7* (D), in 4× and 12× *Dianthus broteri* after exposure to three different temperature range treatments (9/5, 20/18, and 42/28 °C) for 48 h. Values represent the estimated transcript log-abundances ±highest posterior density intervals (n=3). Different letters indicate means that are significantly different from each other (GLM: P<0.05, Tukey's HSD test: α=0.05). In cases where there are significant individual effects of temperature and ploidy but not of their interaction temperature×ploidy, a different set of letters (upper and lower case) is displayed for each cytotype. Asterisks next to factors indicate their level of significance in the model (*P<0.05, **P<0.01, ***P<0.001).

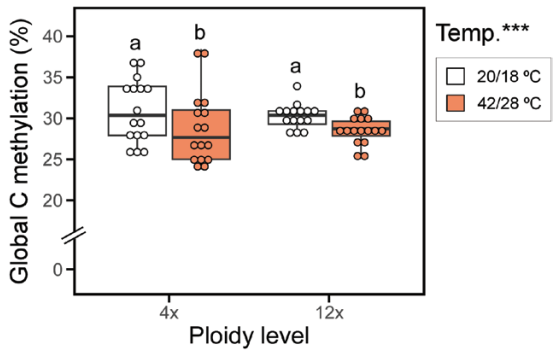

Fig. 5. Global cytosine methylation percentage in 4× and 12× *Dianthus broteri* after exposure to control (20/18 °C) and heat wave (42/28 °C) temperature ranges for 48 h. Both raw data points and box plots are displayed. In the latter, horizontal lines depict the median, and boxes and whiskers represent the interquartile range and the non-outlier ranges, respectively (n=16). Different letters indicate means that are significantly different from each other (LMM: P<0.05, Tukey's HSD test: α=0.05). Asterisks next to factors indicate their level of significance in the model (*P<0.05, **P<0.01, ***P<0.001).

may be a consequence or evidence of more robust photosynthesis in this ploidy relative to 4× (Croft *et al.*, 2017) and could reflect higher biomass accumulation (Sherstneva *et al.*, 2022).

The 4× cytotype suffered higher photoinhibition than 12× under both temperature extremes, but the impact of cold shock was confirmed to be less severe than that of heat shock due to the lower chronic relative to dynamic photoinhibition recorded. Therefore, photochemical damage was mostly reversible in the short term (Osmond and Grace, 1995) after exposure to cold stress. However, the heat treatment caused greater chronic photoinhibition in both cytotypes, but again tetraploids were more acutely affected. Surprisingly, the 4× cytotype exhibited more marked photoprotection mechanisms than 12×, with higher NPQ, which sharply increased under heat.These results together show that dodecaploids use a greater proportion of the excitation energy for photochemical reactions without the need for heat dissipation, allowing them to have a more efficient photosynthesis (Ghosh *et al.*, 2023). This result is undoubtedly indicative of tetraploids being more temperature sensitive than dodecaploids, given that even higher dissipation of excess energy was not able to lower photoinhibition, consequently decreasing photochemical quantum yields and limiting photosynthesis (Haldimann and Feller, 2004).

The higher NPQ of 4× *D. Broteri* was accompanied by a greater activation of the xanthophyll cycle under stress. This cycle consists of the de-epoxidation of violaxanthin to zeaxanthin driven by high energy reaching the thylakoids (which

happens under conditions such as light or temperature stress; Fernández-Marín *et al*., 2021) and is known to greatly contribute to NPQ in higher plants (Murchie and Ruban, 2020). Tetraploids presented reduced epoxidized product (violaxanthin) under heat and cold shocks and, remarkably, a higher DES (a proxy for the activity of the xanthophyll cycle) compared with 12× regardless of temperature. Surprisingly, dodecaploids had greater xanthophyll concentrations (specifically neoxanthin and zeaxanthin) than tetraploids, although in this case it was not supported by NPQ. Due to the high integrity of the photochemical apparatus in 12× *D. broteri*, this result suggests a different role for xanthophylls in photoprotection than in promoting NPQ. Thus, we propose that neoxanthin and zeaxanthin could be acting in dodecaploids as antioxidants, an activity that has already been attributed to these pigments (Havaux *et al.* 2007; Giossi *et al.*, 2020). More elevated neoxanthin concentrations also agreed with higher Chl *b*, the presence of which seems to be a prerequisite for the stable binding of neoxanthin (Voitsekhovskaja and Tyutereva, 2015). In turn, higher Chl *b* in 12× *D. broteri* might be explained by WGD-mediated antenna size enlargement (Kume *et al.*, 2018; and references therein), given that all Chl *b* resides in antenna complexes in land plants.

These complex physiological patterns under temperature stresses are likely to be the intricate outcome of two contributing factors: the direct enlargement effects caused by ploidy increase (additive duplications; as in Mo *et al.*, 2020), and the long-term evolutionary adaptation (Münzbergová and Haisel, 2019) as evidenced in multiple functional traits observed in *D. broteri* (Domínguez-Delgado *et al.*, 2021).

Gene expression and epigenetic changes

As observed in the related species *D. spiculifolius* (Zhou *et al.*, 2017), three out of four stress-related genes selected for *D. broteri* in this study showed differential expression between control and thermal-stressed plants (Fig. 4). Interestingly, differential expression levels with respect to ploidy were detected for all four genes regardless of the temperature regime. Although gene expression should increase linearly after WGD (Stupar *et al.*, 2007), post-polyploidization processes, such as selection, sub- and neo-functionalization, dosage compensation, or epigenetic repatterning, can alter the expected gene expression in polyploids (Chen, 2007). It is therefore remarkable in this study that 12× *D. broteri* presented higher expression than 4× across the four genes, but the absolute gene expression decreased according to the triplication level. Altogether, no inter-cytotype divergence was detected for global DNA methylation under the experimental conditions assayed here (Fig. 5). However, the high inter-population variation in natural levels of global DNA methylation for the 12× cytotype probably due to the influence of specific ecological factors should be noted (Alonso *et al.*, 2016a; Tomczyk *et al.*, 2022). Still, absence of significant differences in this trait should not be interpreted as evidence of similarity in methylation patterns at specific loci because magnitude and patterns of cytosine methylation provide complementary but not identical information (Alonso *et al.*, 2016b). In contrast, the heat treatment significantly decreased global DNA methylation in the two cytotypes, supporting epigenome modulation as a key mechanism in stress response and rapid adaptation to environmental change (Balao *et al.*, 2018; McCaw *et al.*, 2020).

Similarly to gas exchange and water relations, 4× *D. broteri* overall exhibited more marked responses to stress than 12× regarding gene expression. Under heat, tetraploids were able to maintain and increase, respectively, the transcripts of *PP2C16* and *ATHB7*, the latter known to be involved in modulating abscisic acid (ABA) signalling by regulating protein phosphatases such as the former (Valdés *et al.*, 2012). Thus, 4× *D. broteri* showed activated ABA metabolism at high temperatures, a well-known mechanism of plant adaptation to different stresses (Tuteja, 2007). The role of ABA in promoting stomatal closure to reduce water loss aligns with the observed decrease in g_s for the 4× cytotype.

Despite lacking statistical significance, a comparable pattern of up-regulation under heat was observed for *AI5L3*, which is also involved in the ABA signalling pathway (Jing *et al.*, 2020). Dodecaploid *D. broteri* did not show up-regulation of ABA-related genes with heat, but higher basal levels of their transcripts would suggest greater stomatal closure, contrary to the g_s results. The answer to this counterintuitive pattern might be in the responsiveness to ABA. Dodecaploids would have lower ABA sensitivity than tetraploids and hence a more passive control of stomatal opening (Brodribb and McAdam, 2011), allowing them to keep stomata open under stress. This behaviour would facilitate maintaining the photosynthetic activity under stress and an increased capacity for dissipating excess energy through evapotranspiration, as previously stated. Both ambiguous results in polyploid cytotypes regarding ABA signalling and responsiveness have been previously reported for different strains of *Arabidopsis thaliana* (del Pozo and Ramirez-Parra, 2014; Monda *et al.*, 2016).

The expression levels of *SWEET1*, which encodes a sugar transporter, were observed to decrease in response to high temperatures in both cytotypes. Heat stress adversely affects the carbon fixation process and alters the distribution of carbon among various plant organs. Previous studies have reported varying expression patterns of SWEET transporters under heat stress in different species (Gautam *et al.*, 2022). For instance, *SWEET1* was found to be underexpressed in tomato under high temperatures (Peng *et al.*, 2023), whereas it showed increased expression in Arabidopsis (Gautam *et al.*, 2022). Consequently, further investigations are necessary to elucidate the specific role of *SWEET1* under thermal stress in *D. broteri*, and to determine its temperature sensitivity through functional gene studies.

Additionally, the involvement of methylation in the regulation of gene expression for *SWEET6b* (another member of the same family of sugar transporters) under drought conditions has been investigated in rice. It was found that the gene was hypermethylated and up-regulated in response to stress (Wang *et al.*, 2020). While the changes in methylation under abiotic stress such as drought and salinity have been shown to be complex (Zhang *et al.*, 2018), heat stress has been observed to induce active demethylation in specific genes associated with ABA signalling and stress response in Arabidopsis (Korotko *et al.*, 2021). Our study provides further support for the occurrence of widespread cytosine demethylation under heat stress in both cytotypes of *D. broteri*, which is likely to be mediated by enzymes with demethylase activity. This genome-wide demethylation could potentially contribute to the observed alterations in gene expression.

To sum up, our results indicate early divergent physiological performance and resistance, together with altered gene expression and cytosine methylation, in two polyploid cytotypes within the *D. broteri* complex under short thermal stress events. For the higher order cytotype, the combined consequences of ploidy increase (higher cell volume and tissue water storage), and local adaptation (to its particularly stressful environmental niche) would explain its higher photosynthetic performance and ability to cope with high and low temperature extremes. Further research examining the physiological aspects of closely related polyploid taxa will contribute to unravelling their evolutionary dynamics, specifically in relation to factors such as distribution range and competitive interactions. These investigations play a crucial role in advancing our understanding of how climate change may pose challenges to the persistence of plant polyploids.

Supplementary data

The following supplementary data are available at *JXB* online.

Fig. S1. Distribution map of 4× and 12× *Dianthus broteri*, specifying mean annual temperatures of the warmest and coldest quarters.

Fig. S2. Gas exchange parameters (recorded at 300 μmol m^{-2} s^{-1} and 1000 μmol m^{-2} s^{-1} PPFD) in 4× and 12× *Dianthus broteri* cytotypes after exposure to 9/5, 20/18, and 42/28 °C temperature ranges.

Table S1. Description and primer sequences of the genes tested in 4× and 12× *Dianthus broteri*.

Acknowledgements

We thank the Glasshouse, Herbarium, and Biology General Services from the University of Seville for assistance and providing facilities and equipment. We are also grateful to Pilar Bazaga and Esmeralda López for lab assistance, and to three anonymous reviewers for helpful comments on previous versions of the manuscript.

Author contributions

EMN and FB: study design; JLJ, EMN, and FB: carrying out physiological measurements and taking all samples; JPA: conducting the RT-qPCR experiment; CA: conducting the global cytosine methylation experiment; JLJ: data analyses with the supervision of EMN and FB; JLJ: drafting the original manuscript; all authors edited the manuscript before submission and approved the final version.

Conflict of interest

The authors declare no conflicts of interest.

Funding

This work was funded by the Andalusian Government and University of Seville (supported by FEDER funds, FEDER-US-1381232), the Spanish Ministerio de Ciencia e Innovación (Research Project PGC2018-098358-B-I00 and FPI pre-doctoral grant to JP-A), the Fifth Research Plan from the University of Seville (pre-doctoral grant to JL-J), and the Spanish Ministerio de Universidades/NextGenerationEU (Margarita Salas post-doctoral fellowship to J.L-J; University of Seville 289/2021).

Data availability

The data that support the findings of this study are available from the corresponding author upon reasonable request.

References

Abaurrea J, Asín J, Cebrián AC. 2018. Modelling the occurrence of heat waves in maximum and minimum temperatures over Spain and projections for the period 2031–60. Global and Planetary Change **161**, 244–260.

Alonso C, Balao F, Bazaga P, Pérez R. 2016a. Epigenetic contribution to successful polyploidizations: variation in global cytosine methylation along an extensive ploidy series in *Dianthus broteri* (Caryophyllaceae). New Phytologist **212**, 571–576.

Alonso C, Pérez R, Bazaga P, Medrano M, Herrera CM. 2016b. MSAP markers and global cytosine methylation in plants: a literature survey and comparative analysis for a wild-growing species. Molecular Ecology Resources **16**, 80–90.

Baduel P, Quadrana L, Hunter B, Bomblies K, Colot V. 2019. Relaxed purifying selection in autopolyploids drives transposable element over-accumulation which provides variants for local adaptation. Nature Communications **10**, 5818.

Balao F, Casimiro-Soriguer R, Talavera M, Herrera J, Talavera S. 2009. Distribution and diversity of cytotypes in *Dianthus broteri* as evidenced by genome size variations. Annals of Botany **104**, 965–973.

Balao F, Herrera J, Talavera S. 2011. Phenotypic consequences of polyploidy and genome size at the microevolutionary scale: a multivariate morphological approach. New Phytologist **192**, 256–265.

Balao F, Paun O, Alonso C. 2018. Uncovering the contribution of epigenetics to plant phenotypic variation in Mediterranean ecosystems. Plant Biology **20**, 38–49.

Balao F, Valente LM, Vargas P, Herrera J, Talavera S. 2010. Radiative evolution of polyploid races of the Iberian carnation *Dianthus broteri* (Caryophyllaceae). New Phytologist **187**, 542–551.

Bates D, Mächler M, Bolker BM, Walker SC. 2015. Fitting linear mixed-effects models using lme4. Journal of Statistical Software **67**, 1–48.

Bomblies K. 2020. When everything changes at once: finding a new normal after genome duplication. Proceedings of the Royal Society B: Biological Sciences **287**, 20202154.

Brodribb TJ, McAdam SAM. 2011. Passive origins of stomatal control in vascular plants. Science **331**, 582–585.

Čertner M, Sudová R, Weiser M, Suda J, Kolář F. 2019. Ploidy-altered phenotype interacts with local environment and may enhance polyploid establishment in *Knautia serpentinicola* (Caprifoliaceae). New Phytologist **221**, 1117–1127.

Chen ZJ. 2007. Genetic and epigenetic mechanisms for gene expression and phenotypic variation in plant polyploids. Annual Review of Plant Biology **58**, 377–406.

Croft H, Chen JM, Luo X, Bartlett P, Chen B, Staebler RM. 2017. Leaf chlorophyll content as a proxy for leaf photosynthetic capacity. Global Change Biology **23**, 3513–3524.

De Baerdemaeker NJF, Hias N, Van den Bulcke J, Keulemans W, Steppe K. 2018. The effect of polyploidization on tree hydraulic functioning. American Journal of Botany **105**, 161–171.

del Pozo JC, Ramirez-Parra E. 2014. Deciphering the molecular bases for drought tolerance in *Arabidopsis* autotetraploids. Plant, Cell & Environment **37**, 2722–2737.

del Pozo JC, Ramirez-Parra E. 2015. Whole genome duplications in plants: an overview from *Arabidopsis*. Journal of Experimental Botany **66**, 6991–7003.

Domínguez-Delgado JJ, López-Jurado J, Mateos-Naranjo E, Balao F. 2021. Phenotypic diploidization in plant functional traits uncovered by synthetic neopolyploids in *Dianthus broteri*. Journal of Experimental Botany **72**, 5522–5533.

Doyle JJ, Coate JE. 2020. Autopolyploidy: an epigenetic macromutation. American Journal of Botany **107**, 1097–1100.

Duarte B, Goessling JW, Marques JC, Caçador I. 2015a. Ecophysiological constraints of *Aster tripolium* under extreme thermal events impacts: merging biophysical, biochemical and genetic insights. Plant Physiology and Biochemistry **97**, 217–228.

Duarte B, Santos D, Marques JC, Caçador I. 2015b. Impact of heat and cold events on the energetic metabolism of the C_3 halophyte *Halimione portulacoides*. Estuarine, Coastal and Shelf Science **167**, 166–177.

Fernández-Marín B, Roach T, Verhoeven A, García-Plazaola JI. 2021. Shedding light on the dark side of xanthophyll cycles. New Phytologist **230**, 1336–1344.

Fonseca D, Carvalho MJ, Marta-Almeida M, Melo-Gonçalves P, Rocha A. 2016. Recent trends of extreme temperature indices for the Iberian Peninsula. Physics and Chemistry of the Earth, Parts A/B/C **94**, 66–76.

García-Herrera R, Díaz J, Trigo RM, Luterbacher J, Fischer EM, Garcia-Herrera R, Díaz J, Trigo RM, Luterbacher J, Fischer EM. 2010. A review of the European summer heat wave of 2003. Critical Reviews in Environmental Science and Technology **40**, 267–306.

Gautam T, Dutta M, Jaiswal V, Zinta G, Gahlaut V, Kumar S. 2022. Emerging roles of SWEET sugar transporters in plant development and abiotic stress responses. Cells **11**, 1303.

Genty B, Briantais J-M, Baker NR. 1989. The relationship between the quantum yield of photosynthetic electron transport and quenching of chlorophyll fluorescence. Biochimica et Biophysica Acta **990**, 87–92.

Ghosh D, Mohapatra S, Dogra V. 2023. Improving photosynthetic efficiency by modulating non-photochemical quenching. Trends in Plant Science **28**, 264–266.

Giorgi F, Lionello P. 2008. Climate change projections for the Mediterranean region. Global and Planetary Change **63**, 90–104.

Giossi C, Cartaxana P, Cruz S. 2020. Photoprotective role of neoxanthin in plants and algae. Molecules **25**, 4617.

Grassi B, Redaelli G, Visconti G. 2013. Arctic sea ice reduction and extreme climate events over the Mediterranean region. Journal of Climate **26**, 10101–10110.

Greer BT, Still C, Cullinan GL, Brooks JR, Meinzer FC. 2017. Polyploidy in fluences plant–environment interactions in quaking aspen (*Populus tremuloides* Michx). Tree Physiology **38**, 630–640.

Grossiord C, Buckley TN, Cernusak LA, Novick KA, Poulter B, Siegwolf RTW, Sperry JS, McDowell NG. 2020. Plant responses to rising vapor pressure deficit. New Phytologist **226**, 1550–1566.

Haldimann P, Feller U. 2004. Inhibition of photosynthesis by high temperature in oak (*Quercus pubescens* L) leaves grown under natural conditions closely correlates with a reversible heat-dependent reduction of the activation state of ribulose-1,5-bisphosphate carboxylase/oxygenase. Plant, Cell & Environment **27**, 1169–1183.

Hao G-Y, Lucero ME, Sanderson SC, Zacharias EH, Holbrook NM. 2013. Polyploidy enhances the occupation of heterogeneous environments through hydraulic related trade-offs in *Atriplex canescens* (Chenopodiaceae). New Phytologist **197**, 970–978.

Havaux M, Dall'Osto L, Bassi R. 2007. Zeaxanthin has enhanced antioxidant capacity with respect to all other xanthophylls in *Arabidopsis* leaves and functions independent of binding to PSII antennae. Plant Physiology **145**, 1506–1520.

He Z, Webster S, He SY. 2022. Growth–defense trade-offs in plants. Current Biology **32**, R634–R639.

Hendrickson L, Chow WS, Furbank RT. 2004. Low temperature effects on grapevine photosynthesis: the role of inorganic phosphate. Functional Plant Biology **31**, 789–801.

Jing D, Chen W, Xia Y, Shi M, Wang P, Wang S, Wu D, He Q, Liang G, Guo Q. 2020. Homeotic transformation from stamen to petal in *Eriobotrya japonica* is associated with hormone signal transduction and reduction of the transcriptional activity of *EjAG*. Physiologia Plantarum **168**, 893–908.

Koloušková P, Stone JD, Štorchová H. 2017. Evaluation of reference genes for reverse transcription quantitative real-time PCR (RT–qPCR) studies in *Silene vulgaris* considering the method of cDNA preparation. PLoS One **12**, e0183470.

Korotko U, Chwiałkowska K, Sańko-Sawczenko I, Kwasniewski M. 2021. DNA demethylation in response to heat stress in *Arabidopsis thaliana*. International Journal of Molecular Sciences **22**, 1555.

Kume A, Akitsu T, Nasahara KN. 2018. Why is chlorophyll *b* only used in light-harvesting systems? Journal of Plant Research **131**, 961–972.

Küpper H, Seibert S, Parameswaran A. 2007. Fast, sensitive, and inexpensive alternative to analytical pigment HPLC: quantification of chlorophylls and carotenoids in crude extracts by fitting with Gauss peak spectra. Analytical Chemistry **79**, 7611–7627.

Landis JB, Soltis DE, Li Z, Marx HE, Barker MS, Tank DC, Soltis PS. 2018. Impact of whole-genome duplication events on diversification rates in angiosperms. American Journal of Botany **105**, 348–363.

Lau NC, Nath MJ. 2014. Model simulation and projection of European heat waves in present-day and future climates. Journal of Climate **27**, 3713–3730.

Lawson T, Vialet-Chabrand S. 2019. Speedy stomata, photosynthesis and plant water use efficiency. New Phytologist **221**, 93–98.

Levin DA, Soltis DE. 2018. Factors promoting polyploid persistence and diversification and limiting diploid speciation during the K–Pg interlude. Current Opinion in Plant Biology **42**, 1–7.

Li WL, Berlyn GP, Ashton PMS. 1996. Polyploids and their structural and physiological characteristics relative to water deficit in *Betula papyrifera* (Betulaceae). American Journal of Botany **83**, 15–20.

Liao T, Wang Y, Xu CP, Li Y, Kang XY. 2018. Adaptive photosynthetic and physiological responses to drought and rewatering in triploid Populus populations. Photosynthetica **56**, 578–590.

López-Jurado J, Balao F, Mateos-Naranjo E. 2016. Deciphering the ecophysiological traits involved during water stress acclimation and recovery of the threatened wild carnation, *Dianthus inoxianus*. Plant Physiology and Biochemistry **109**, 397–405.

López-Jurado J, Balao F, Mateos-Naranjo E. 2020. Polyploidy-mediated divergent light-harvesting and photoprotection strategies under

temperature stress in a Mediterranean carnation complex. Environmental and Experimental Botany **171**, 103956.

López-Jurado J, Mateos-Naranjo E, Balao F. 2019a. Niche divergence and limits to expansion in the high polyploid *Dianthus broteri* complex. New Phytologist **222**, 1076–1087.

López-Jurado J, Mateos-Naranjo E, Balao F. 2022. Polyploidy promotes divergent evolution across the leaf economics spectrum and plant edaphic niche in the *Dianthus broteri* complex. Journal of Ecology **110**, 605–618.

López-Jurado J, Mateos-Naranjo E, García-Castaño JL, Balao F. 2019b. Conditions for translocation of a key threatened species, *Dianthus inoxianus* Gallego, in the southwestern Iberian Mediterranean forest. Forest Ecology and Management **446**, 1–9.

Losada JM, Blanco-Moure N, Fonollá A, Martínez-Ferrí E, Hormaza JI. 2023. Hydraulic tradeoffs underlie enhanced performance of polyploid trees under soil water deficit. Plant Physiology **192**, kiad204.

Madlung A, Wendel JF. 2013. Genetic and epigenetic aspects of polyploid evolution in plants. Cytogenetic and Genome Research **140**, 270–285.

Maherali H, Walden AE, Husband BC. 2009. Genome duplication and the evolution of physiological responses to water stress. New Phytologist **184**, 721–731.

Martinez-Vilalta J, Anderegg WRL, Sapes G, Sala A. 2019. Greater focus on water pools may improve our ability to understand and anticipate drought-induced mortality in plants. New Phytologist **223**, 22–32.

Matz MV. 2020. MCMC.qpcr: Bayesian analysis of qRT-PCR data. R package version 1.2.4. https://CRAN.R-project.org/package=MCMC.qpcr

Matz MV, Wright RM, Scott JG. 2013. No control genes required: Bayesian analysis of qRT-PCR data. PLoS One **8**, e71448.

McCaw BA, Stevenson TJ, Lancaster LT. 2020. Epigenetic responses to temperature and climate. Integrative and Comparative Biology **60**, 1469–1480.

Mizokami Y, Sugiura D, Watanabe CKA, Betsuyaku E, Inada N, Terashima I. 2019. Elevated CO_2-induced changes in mesophyll conductance and anatomical traits in wild type and carbohydrate-metabolism mutants of *Arabidopsis*. Journal of Experimental Botany **70**, 4807–4818.

Mo L, Chen J, Lou X, Xu Q, Dong R, Tong Z, Huang H, Lin E. 2020. Colchicine-induced polyploidy in *Rhododendron fortunei* Lindl. Plants (Basel, Switzerland) **9**, 424.

Monda K, Araki H, Kuhara S, *et al*. 2016. Enhanced stomatal conductance by a spontaneous *Arabidopsis* tetraploid, Me-0, results from increased stomatal size and greater stomatal aperture. Plant Physiology **170**, 1435–1444.

Moura RF, Queiroga D, Vilela E, Moraes AP. 2021. Polyploidy and high environmental tolerance increase the invasive success of plants. Journal of Plant Research **134**, 105–114.

Münzbergová Z, Haisel D. 2019. Effects of polyploidization on the contents of photosynthetic pigments are largely population-specific. Photosynthesis Research **140**, 289–299.

Murchie EH, Ruban AV. 2020. Dynamic non-photochemical quenching in plants: from molecular mechanism to productivity. The Plant Journal **101**, 885–896.

Osmond CB, Grace SC. 1995. Perspectives on photoinhibition and photorespiration in the field: quintessential inefficiencies of the light and dark reactions of photosynthesis? Journal of Experimental Botany **46**, 1351–1362.

Pacey EK, Maherali H, Husband BC. 2022. Polyploidy increases storage but decreases structural stability in *Arabidopsis thaliana*. Current Biology **32**, 4057–4063.e3.

Parisod C, Holderegger R, Brochmann C. 2010. Evolutionary consequences of autopolyploidy. New Phytologist **186**, 5–17.

Peng C, Shu S, Wang Y, Du J, Shi L, Jahan MS, Guo S. 2023. Transcriptome analysis of the regulatory mechanism of exogenous spermidine in high temperature stress resistance of tomato seedlings. Agronomy **13**, 285.

Pérez-Romero JA, Barcia-Piedras J-M, Redondo-Gómez S, Mateos-Naranjo E. 2019. Impact of short-term extreme temperature events on physiological performance of *Salicornia ramosissima* J Woods under optimal and sub-optimal saline conditions. Scientific Reports **9**, 659.

Pérez-Romero JA, Mateos-Naranjo E, López-Jurado J, Redondo-Gómez S, Torres-Ruiz JM. 2020. Importance of physiological traits vulnerability in determine halophytes tolerance to salinity excess: a comparative assessment in *Atriplex halimus*. Plants **9**, 690.

Pintó-Marijuan M, Munné-Bosch S. 2013. Ecophysiology of invasive plants: osmotic adjustment and antioxidants. Trends in Plant Science **18**, 660–666.

Rakić T, Gajić G, Lazarević M, Stevanović B. 2015. Effects of different light intensities, CO_2 concentrations, temperatures and drought stress on photosynthetic activity in two paleoendemic resurrection plant species *Ramonda serbica* and *R. nathaliae*. Environmental and Experimental Botany **109**, 63–72.

Ramsey J, Schemske DW. 1998. Pathways, mechanisms, and rates of polyploid formation in flowering plants. Annual Review of Ecology and Systematics **29**, 467–501.

R Core Team. 2020. R: a language and environment for statistical computing. Vienna, Austria: R Foundation for Statistical Computing.

Rey PJ, Manzaneda AJ, Alcántara JM. 2017. The interplay between aridity and competition determines colonization ability, exclusion and ecological segregation in the heteroploid *Brachypodium distachyon* species complex. New Phytologist **215**, 85–96.

Rice A, Šmarda P, Novosolov M, Drori M, Glick L, Sabath N, Meiri S, Belmaker J, Mayrose I. 2019. The global biogeography of polyploid plants. Nature Ecology and Evolution **3**, 265–273.

Rodríguez-Parra A, Picazo-Aragonés J, Balao F. 2022. Evaluation of reference genes in the polyploid complex *Dianthus broteri* (Caryophyllaceae) using qPCR. Plants (Basel, Switzerland) **11**, 518.

Sage RF, Way DA, Kubien DS. 2008. Rubisco, Rubisco activase, and global climate change. Journal of Experimental Botany **59**, 1581–1595.

Sánchez-Benítez A, García-Herrera R, Barriopedro D, Sousa PM, Trigo RM. 2018. June 2017: the earliest European summer mega-heatwave of reanalysis period. Geophysical Research Letters **45**, 1955–1962.

Scafaro AP, Gallé A, Van Rie J, Carmo-Silva E, Salvucci ME, Atwell BJ. 2016. Heat tolerance in a wild *Oryza* species is attributed to maintenance of Rubisco activation by a thermally stable Rubisco activase ortholog. New Phytologist **211**, 899–911.

Scaife A, Knight J. 2008. Ensemble simulations of the cold European winter of 2005–2006. Quarterly Journal of the Royal Meteorological Society **134**, 1647–1659.

Schreiber U, Schliwa U, Bilger W. 1986. Continuous recording of photochemical and non-photochemical chlorophyll fluorescence quenching with a new type of modulation fluorometer. Photosynthesis Research **10**, 51–62.

Schymanski SJ, Or D, Zwieniecki M. 2013. Stomatal control and leaf thermal and hydraulic capacitances under rapid environmental fluctuations. PLoS One **8**, e54231.

Sherstneva O, Khlopkov A, Gromova E, Yudina L, Vetrova Y, Pecherina A, Kuznetsova D, Krutova E, Sukhov V, Vodeneev V. 2022. Analysis of chlorophyll fluorescence parameters as predictors of biomass accumulation and tolerance to heat and drought stress of wheat (*Triticum aestivum*) plants. Functional Plant Biology **49**, 155–169.

Spoelhof JP, Soltis PS, Soltis DE. 2017. Pure polyploidy: closing the gaps in autopolyploid research. Journal of Systematics and Evolution **55**, 340–352.

Stull GW, Qu XJ, Parins-Fukuchi C, *et al*. 2021. Gene duplications and phylogenomic conflict underlie major pulses of phenotypic evolution in gymnosperms. Nature Plants **7**, 1015–1025.

Stupar RM, Bhaskar PB, Yandell BS, *et al*. 2007. Phenotypic and transcriptomic changes associated with potato autopolyploidization. Genetics **176**, 2055–2067.

Tomczyk PP, Kiedrzyński M, Forma E, Zielińska KM, Kiedrzyńska E. 2022. Changes in global DNA methylation under climatic stress in two related grasses suggest a possible role of epigenetics in the ecological success of polyploids. Scientific Reports **12**, 8322.

Tuteja N. 2007. Abscisic acid and abiotic stress signaling. Plant Signaling & Behavior **2**, 135–138.

Valdés AE, Övernäs E, Johansson H, Rada-Iglesias A, Engström P. 2012. The homeodomain-leucine zipper (HD-Zip) class I transcription factors ATHB7 and ATHB12 modulate abscisic acid signalling by regulating protein phosphatase 2C and abscisic acid receptor gene activities. Plant Molecular Biology **80**, 405–418.

Van De Peer Y, Ashman T-L, Soltis PS, Soltis DE. 2021. Polyploidy: an evolutionary and ecological force in stressful times. The Plant Cell **33**, 11–26.

Voitsekhovskaja OV, Tyutereva EV. 2015. Chlorophyll *b* in angiosperms: functions in photosynthesis, signaling and ontogenetic regulation. Journal of Plant Physiology **189**, 51–64.

Wang G, Li H, Meng S, Yang J, Ye N, Zhang J. 2020. Analysis of global methylome and gene expression during carbon reserve mobilization in stems under soil drying. Plant Physiology **183**, 1809–1824.

Wang L, Cao S, Wang P, Lu K, Song Q, Zhao F-J, Chen ZJ. 2021. DNA hypomethylation in tetraploid rice potentiates stress-responsive gene expression for salt tolerance. Proceedings of the National Academy of Sciences, USA **118**, e2023981118.

Werner C, Correia O, Beyschlag W. 2002. Characteristic patterns of chronic and dynamic photoinhibition of different functional groups in a Mediterranean ecosystem. Functional Plant Biology **29**, 999–1011.

Yu W, Tao Y, Luo L, Hrovat J, Xue A, Luo H. 2021. Evaluation of housekeeping gene expression stability in carnation (*Dianthus caryophyllus*). New Zealand Journal of Crop and Horticultural Science **49**, 347–360.

Zhang H, Lang Z, Zhu J-K. 2018. Dynamics and function of DNA methylation in plants. Nature Reviews, Molecular Cell Biology **19**, 489–506.

Zhou A, Ma H, Liu E, Jiang T, Feng S, Gong S, Wang J. 2017. Transcriptome sequencing of *Dianthus spiculifolius* and analysis of the genes involved in responses to combined cold and drought stress. International Journal of Molecular Sciences **18**, 849.